DARU Journal of Pharmaceutical Sciences
https://doi.org/10.1007/s40199-020-00355-8

RESEARCH ARTICLE

Stabilized oral nanostructured lipid carriers of Adefovir Dipivoxil as a potential liver targeting: Estimation of liver function panel and uptake following intravenous injection of radioiodinated indicator

Shady M. Abd El-Halim[1] · Ghada A. Abdelbary[2] · Maha M. Amin[2] · Mohamed Y. Zakaria[3] · Hesham A. Shamsel-Din[4] · Ahmed B. Ibrahim[4]

Received: 19 October 2019 / Accepted: 15 June 2020

Abstract

Purpose Adefovir dipivoxil (AD), a nucleoside reverse transcriptase inhibitor is effective against Hepatitis B virus. Its poor oral bioavailability leads to frequent administration causing severe adverse effects. Thereby the entrapment of AD within lipid nanoparticulate systems is a way of increasing AD oral bioavailability as a result of improving intestinal permeability with efficient liver-targeted delivery together with higher drug stability during storage.

Methods AD-loaded nanostructured lipid carriers (AD-NLCs) were prepared via solvent emulsification diffusion technique adopting 2^4 full factorial design to study the effect of lipid percentage, presence of egg yolk lecithin, surfactant type and percentage on entrapment efficiency (E.E.%), particle size and percent in-vitro drug released after 8 h (Q8hrs).

Results Formula (F12) showed E.E.% of 90.5 ± 0.2%, vesicle size of 240.2 ± 2.5 nm and Q8hrs of 58.55 ± 9.4% was selected as the optimum formula with desirability value of 0.757 based on highest EE%, lowest P.S. and Q8hrs. Further evaluation of the optimized formula using radioiodinated rose bengal (RIRB) in thioacetamide induced liver damage in Swiss Albino mice revealed a higher liver uptake of 22 ± 0.01% ID/g (percent injected dose/g organ) and liver uptake/Blood (T/B) ratio of 2.22 ± 0.067 post 2 h of I.V injection of RIRB compared to 9 ± 0.01% ID/g and 0.64 ± 0.017 in untreated group, respectively.

Conclusion NLCs could be successfully used as oral drug delivery carriers of the antiviral drug Adefovir Dipivoxil to the liver with higher stability and oral bioavailability.

Keywords Adefovir dipivoxil · Nanostructured lipid carrier · Thiocetamide induced liver damage · Radioiodinated rose bengal · Biodistribution study

Introduction

Liver diseases have been considered as the most worldwide health problems resulting in significantly high morbidity and mortality. The primary causative factors for developing of such diseases are environmental toxins, parasitic diseases, drugs predisposed to hepato-toxicity as (thioacetamide, carbon tetrachloride, chemotherapeutic agents and high doses of paracetamol) and viruses induced hepatitis B and C [1].

Our candidate drug Adefovir Dipivoxil (AD) is an antiviral prodrug belongs to nucleoside analogue class exerting its antiviral activity via inhibition of reverse transcriptase enzyme. Furthermore, AD was reported to effectively maintain liver histology and normalize liver function enzymes as serum

✉ Shady M. Abd El-Halim
shady_mohammed@o6u.edu.eg

[1] Department of Pharmaceutics and Industrial Pharmacy, Faculty of Pharmacy, October 6 University, Central Axis, 6th of October City, Giza 12585, Egypt

[2] Department of Pharmaceutics and Industrial Pharmacy, Faculty of Pharmacy, Cairo University, Cairo 11562, Egypt

[3] Department of Pharmaceutics and Industrial Pharmacy, Faculty of Pharmacy and Pharmaceutical Industry, Port Said University, Port said 42526, Egypt

[4] Department of Labeled Compounds, Hot Labs Center, Egyptian Atomic Energy Authority, Cairo 13759, Egypt

Published online: 20 June 2020

alanine aminotransferase (ALT) level [2, 3]. Unfortunately the ionization of the phosphonate moiety of AD prompts the diminishing of its oral bioavailability like other antivirals, thereby hindering its ability to cross intestinal epithelium [4]. In addition, being P-glycoprotein (P-gp) substrate, this leads to further reduction in its oral bioavailability. Therefore, administration of larger or multiple doses is required to hit the effective concentration of the drug causing severe adverse effects leading to a great negative impact on patient compliance [5].

In the past decade, vast investigations and experimental trials were conducted on the utilization of nanomedicine aiming to overcome drug associated problems regarding solubility and bioavailability. The formulation of nanoparticulate carrier systems gasp the attention of various scientists in order to enhance the drugs oral bioavailability [6]. Such studies, fabrication of Adefovir dipivoxil proliposomal powders, polymeric nanoparticles and solid lipid nanoparticles that succeeded to improve its bioavailability and biodistribution [5, 7].

Various drawbacks were noticed regarding polymeric nanoparticles such as inability to scale up its production and its toxicity [8]. Despite SLNs as safe carriers being biocompatible and biodegradable, drug ejection during storage and the lower drug charging capacity were the major drawbacks as the particles in the solid lipid matrix were aligned as closely packed supreme perfect crystal grid permitting lower voids to keep the drug which hinders the charging capacity and leads to an increase in drug ejection [9].

Nanostructured lipid carriers (NLCs) as a second wave of SLNs have been evolved, compromising both solid lipid and liquid lipid (oil) matrix, hence initiating less organized structures possessing the feature of diminishing the delocalization of the encapsulated drug and improving the drug charging ability [10].

In addition to higher drug loading capacity, NLCs are characterized by being superior over other traditional carriers regarding boosting the solubility of lipophilic drugs, imparting controlled and sustained drug release characteristics, enhancing drug permeability suitable for tissue-targeted delivery with lessen adverse effects. In addition, drug-loaded NLCs could reduce chemical or enzymatic degradation of drugs being embedded in the lipid forge, thereby maintaining higher drug stability during storage [9, 11, 12].

The composition of NLC with its solid and liquid lipids is such like a diet enriched with fat. During GIT digestion, these lipids have the ability to impel the bile secretion in the small intestinal when orally ingested and then the NLCs loaded with the drug were coupled with bile salts to form mixed micelles [13]. This process augmented the intact NLCs to be transferred directly to portal blood through paracellular route or being gripped by M cells evading the first pass metabolism and thus promoting the lymphatic transport resulting in higher oral bioavailability [9, 14]. Recent researchers approved that NLCs containing specific surfactants and lipids could efficiently avoid the efflux by P-gp, thereby could enhance drug absorption [15].

Rose bengal (RB) is an artificial fabricated dye adopted in the apparel industry, was first introduced in 1882 and it has a lot of applications in the medical scope as a diagnostic tool in ocular infections, a stain for corneal ulceration and as a measure of hepatic function [16, 17]. Rose bengal is selectively picked up by normal hepatocytes following its intravenous injection, it rapidly circulates and localizes in the liver and then rapidly excreted into the biliary system [18, 19]. Changes in radioactivity in blood have been assumed to reflect the removal of RB by the liver resulting in higher liver uptake/blood ratio, while in case of diseased livers, the liver uptake of RB will be decreased significantly and accordingly the liver uptake/blood ratio will be diminished. The labeling of this dye with a gamma emitting isotope (^{131}I) facilitates its tracking as radioiodinated rose bengal indicator (RIRB) to monitor and evaluate its liver uptake and clearance to be useful in the assessment of hepatic function [20–24].

In the current study, AD-loaded NLCs were fabricated, via solvent emulsification diffusion tactic [25], aiming to improve both bioavailability and liver targeting of AD following oral administration. The executed in-vivo study in mice estimated the capability of the optimum formula loaded with AD to shelter the liver against hepatic damage prompted chemically utilizing thioacetamide (TAA) by measurement of RIRB liver uptake in both treated and untreated groups.

Materials and methods

Materials

Adefovir Dipivoxil (AD) was kindly supplied by EVA Pharmaceutical Co., Cairo, Egypt. Cremophor RH 40, Pluronic F68 (Poloxamer 188), egg yolk L-α-phosphatidylcholine (PC) (Lecithin), rose bengal, thioacetamide (TAA), potassium iodate (KIO_3), tetrahydrofuran (THF) and Whatman paper no. 1 were purchased from Sigma Chemical Co. St. Louis, MO, USA. Geleol, Gelucire 50/13, Precirol ATO-5 (glyceryl palmostearate), Gelucire 44/14, Compritol 888 (glyceryl behenate), Capryol-90, Capmul MCM, Labrasol, Labrafil M212 and Labrafac lipophile were received as gift from Gattefosse (France). Sodium chloride, potassium dihydrogen orthophosphate, methanol, sodium hydroxide, magnesium chloride, and absolute ethanol were obtained from El-Gomhouria Chemical Co., Cairo, Egypt. Dialysis membrane (Spectra/Pore®, cut off 12,000-14,000) was purchased from Spectrum Laboratories Inc., USA). No-carrier added sodium iodide (NCA $Na^{131}I$, 3.7 GBq/mL), Radioisotope Production Factory (RPF), Egypt Atomic Energy Authority (EAEA), Egypt.

Lipid screening and selection of lipid matrix

Solid lipids (1 g of Geleol, Gelucire 50/13, Precirol ATO-5, Gelucire 44/14 and Compritol 888) was kept individually at temperature 5 °C above the melting point of lipids in a shaking water bath (Model 25, Precision scientific) up to 48 h. About 10 mg increment of AD was added to each one and homogenously distributed using a vortex mixer until excess AD remained undissolved, hence, the saturation occurred and the amount of dissolved AD was recorded directly. Also, the solubility of AD in liquid lipids (oils as Capryol-90, Capmul MCM, Labrasol, Labrafil M212 and Labrafac lipophile) was detected after centrifugation at 15000 rpm and 25 °C for 40 min in order to separate the undissolved AD. The detection of the concentration of AD was done spectrophotometrically (Shimadzu, model UV-1601 PC, Kyoto, Japan) at λ_{max} 260 nm [26].

Preparation of AD-loaded NLCs

The selected variables were lipid mixture percentage (2 or 5%*w/v*), surfactant type (Cremophor RH40 or Pluronic F68), surfactant percentage (1 or 3% w/v) and presence or absence of egg yolk lecithin (1% w/v). The lipid matrix composed of Precirol ATO-5 as the solid lipid and Capmul MCM as oil in a ratio of (3:1). The impact of these variables on the constructed NLCs loaded with AD was investigated utilizing a full factorial design (2^4). The appraised responses were: Percent entrapment efficiency (E.E%), percent in-vitro released after 8 h (Q8hrs) and particle size determination. For that, sixteen experiments are fabricated and summarized in (Table 1).

Briefly, the predetermined quantities of Precirol ATO-5, egg yolk PC (if present) and Capmul MCM were dissolved in THF along with AD resembling the organic phase, which was infused slowly to an aqueous phase enclosing a specified amount of a surfactant (Cremophor RH40 or Pluronic F68) under stirring. The produced primary O/W emulsion was subjected to ultrasonication using probe sonicator for 10 min at 60% amplitude (Model 275 T Crest Ultrasonics Corp., Trenton, NJ). Finally the resulting emulsion was kept under continuous stirring (MS-300HS, Misung Scientific Co., Korea) to permit the complete evaporation of the organic solvent and the precipitation of AD-NLCs [27].

In-vitro characterization of the prepared AD-loaded NLCs

Entrapment efficiency percent (E.E%)

As a mean to estimate the percentage of AD enclosed within the prepared NLCs, accurately; 1 ml of AD-loaded NLC dispersion (resembling 5 mg of the drug) diluted with 5 mL distilled water and manually shacked for 2 min. The unentrapped drug was decoupled from AD-loaded NLC by cooling centrifugation technique for one hour at 15,000 rpm and 4 °C (Beckman, Fullerton, Canada). The settled nanoparticles were collected away, rinsed twice with distilled and recentrifuged again for 30 min. The sonication of the separated particles using methanol was performed to detect the amount of the encapsulated AD [28]. The concentration of the enclosed AD within the particles was detected spectrophotometrically at λ_{max} 260 nm versus methanol as blank. (E.E%) was calculated as follows:

$$\%AD\ Entrapped = (Amount\ of\ AD\ entrapped / Total\ amount\ of\ AD) X 100 \quad (1)$$

Vesicle size, zeta potential and polydispersity index (PDI) determination

Mastersizer (Malvern Instruments, Malvern, UK) was utilized to evaluate the droplet size, zeta potential and PDI of the prepared AD-loaded NLCs. The dilution of 0.1 mL of AD-loaded NLC formula with aliquot of 10 mL distilled water in a glass tube was performed and shacked manually for 5 min. Laser diffraction technique was used to determine the distribution size at 25 °C using 45 mm focus lens and beam length of 2.4 mm. The test was performed in triplicates [26].

In-vitro AD release

About 1 mL of each of the prepared AD-loaded NLC formulae was diluted to 5 mL sorensen phosphate buffer (pH 7.4), then (1 mL) equivalent to 1 mg AD from the diluted particle dispersion was conveyed to a 10 cm in length and 2.5 cm in diameter glass cylinder and a presoaked cellulose membrane was placed at its bottom where the dispersion was prevalenced over. The glass cylinder was mounted on the shaft of the dissolution tester (Copley, DIS 8000, Nottingham, UK) and suspended in 500 mL dissolution media (sorensen phosphate buffer, pH 7.4) at 37 ± 0.5 °C and speed of 50 rpm [29]. At designated time interventions, equal volumes were withdrawn and the percent drug released was detected spectrophotometrically at 260 nm. In-vitro AD release was carried out in triplicates.

Based on the minimum globule size, Q8hrs and maximum E.E%, the optimum AD nanoparticle formula was selected. Statistical analysis of the data was performed using Design Expert® 7 software (Stateese, Minneapolis, USA) and the best formula with the elevated desirability value was picked for furthermore evaluations.

Table 1 Composition of the different prepared AD-loaded NLCs with their corresponding dependant variables

Formulae	Lipid mixture concentration (% *w/v*)	S.A.A concentration (% w/v)	S.A.A type	Lecithin (Absent /present)	E.E (%) ±S.D	Particle size (nm) ±S.D	PDI ± S.D	Zeta potential (mV) ± S.D	Q8hrs (%) ± S.D
F1	2	1	Cremophor RH40	A	29.60 ± 0.5	132.50 ± 11.2	0.35 ± 0.1	−18.95 ± 2.5	87.70 ± 4.9
F2	2	1	Cremophor RH40	P	34.70 ± 2.4	179.10 ± 12.3	0.285 ± 0.0	−22.65 ± 0.5	65.92 ± 0.9
F3	5	1	Cremophor RH40	A	45.30 ± 1.1	156.00 ± 4.1	0.36 ± 0.1	−16.30 ± 0.4	66.31 ± 1.9
F4	5	1	Cremophor RH40	P	55.05 ± 1.6	202.50 ± 8.4	0.42 ± 0.9	−17.62 ± 0.6	69.45 ± 3.5
F5	2	3	Cremophor RH40	A	5.53 ± 0.2	59.15 ± 1.1	0.53 ± 0.1	−12.65 ± 0.9	49.43 ± 7.4
F6	2	3	Cremophor RH40	P	7.95 ± 0.2	121.00 ± 12.7	0.45 ± 0.2	−17.81 ± 0.8	94.85 ± 12.6
F7	5	3	Cremophor RH40	A	27.30 ± 5.5	139.52 ± 16.2	0.26 ± 0.1	−17.25 ± 0.3	98.20 ± 4.9
F8	5	3	Cremophor RH40	P	50.35 ± 1.3	210.51 ± 12.4	0.57 ± 0.2	−18.95 ± 0.4	43.51 ± 7.9
F9	2	1	Pluronic F68	A	35.95 ± 1.7	470.60 ± 16.5	0.49 ± 0.8	−22.43 ± 0.9	57.94 ± 7.5
F10	2	1	Pluronic F68	P	77.50 ± 1.5	599.33 ± 17.5	0.47 ± 0.7	−22.20 ± 0.3	43.85 ± 7.4
F11	5	1	Pluronic F68	A	69.93 ± 1.6	208.82 ± 24.6	0.38 ± 0.0	−7.89 ± 1.1	53.00 ± 4.9
F12	5	1	Pluronic F68	P	90.55 ± 0.2	240.20 ± 2.5	0.21 ± 0.08	−8.32 ± 0.4	58.55 ± 9.4
F13	2	3	Pluronic F68	A	42.55 ± 0.7	144.71 ± 5.6	0.34 ± 0.1	−8.15 ± 1.1	75.75 ± 7.9
F14	2	3	Pluronic F68	P	64.65 ± 3.0	274.32 ± 10.2	0.25 ± 0.1	−13.30 ± 0.1	48.00 ± 3.9
F15	5	3	Pluronic F68	A	33.98 ± 3.8	823.01 ± 44.2	0.56 ± 0.2	−20.75 ± 1.7	33.55 ± 5.3
F16	5	3	Pluronic F68	P	52.80 ± 2.7	940.00 ± 59.8	0.49 ± 0.2	−26.45 ± 0.2	54.15 ± 5.3

*Each formula contains 10 mg adefovir dipivoxil

In-vitro characterization of the optimum lyophilized AD-loaded NLC formula

The optimum AD-loaded NLC formula was solidified via freeze-drying technique (Alpha 2–4, CHRIST, Osterode am Harz, Germany), where lysis of the nanoparticles was hindered using mannitol (5% *w/v*) as lyoprotectant. Furthermore, NLC suspension was freezed over night at −80 °C and dried for a period of 24 h under vacuum [30]. The freeze-dried NLC powder was kept in a firmly closed glass tubes in a desiccator for furthermore analysis.

Differential scanning calorimetry (DSC)

Differential scanning calorimeter (DSC-50, Shimadzu, Kyoto, Japan) was used to evaluate the thermal attitude of pure AD, optimum formula, Precirol ATO-5, Pluronic F68. Purified indium (99.9%) was used to calibrate the equipment. Around (3 mg) samples were incorporated on the equipped aluminum pans and heated provided that 10 °C was elevated each minute, surrounded by nitrogen in a temperature range of 20 – 400 °C.

X-ray diffractometry (XRD)

The crystallinity of the pure drug in the desired formula was evaluated and analyzed by X-ray diffractometer (XGEN-4000, Scintag Corp., Sunnyvale, CA). Ni-filtered Cu Ka radiation at 40 mA current and 45 kV Voltage was allowed to access the samples. Diffraction patterns recorded the X-ray intensity as a function of 2θ angle covering from 2.0° to 50.0°. The scanning rate was 6°/minute.

Transmission electron microscope (TEM)

Transmission electron microscope was used to investigate the morphology of the optimum lyophilized AD-loaded NLC formula after its dilution with distilled water. A drop (2 μL) was withdrawn from the dispersion and was settled on a carbon-coated copper grid and dried in presence of bright light until the formation of a thin liquid film on one side. This sheet of copper with the stained film was placed onto the end of a long iron bar and inserted into the TEM for photography [26].

Stability study

A comparative stability study between the freeze-dried and non-freeze-dried formulations of the desired drug loaded NLC formula was conducted at the end of 6 months storage period. Sealed amber colored glass vials were used to store the formulae in refrigerator at a temperature of about 4 ± 2 °C. The stored formulae were assessed with respect to encapsulation efficiency, *Q8hrs*, globule size and polydispersity and compared to the freshly prepared formula [31].

In-vivo characterization of the desired lyophilized AD-charged NLC formula

Preparation of radioiodinated rose bengal indicator

Different techniques for the preparation of RIRB have been conducted either by chemical synthesis or isotopic exchange reaction in aqueous or organic media at temperatures between 50 and 120 °C and reaction time between 1 to 12 h [32, 33].

In our study, the radioiodination process was performed via isotopic exchange mechanism as follows; one mL of ethanolic solution containing 1–10 mg of highly purified RB, 0.06 mL 1 M HCl, and 0.5 mL of freshly prepared oxidizing agent solution in distilled water containing 100–600 μg of KIO_3 were kept in a well stoppered vial followed by gentle shaking for 5 min. Using a 1 mL syringe and needle, 100 μl of $Na^{131}I$ (7.4 MBq) was added to the acidified ethanol RB-KIO_3 solution. The reaction mixture was then transferred to a water bath at different temperatures for different time intervals (5–60 min) to allow the exchange reaction to be completed and obtained the highest radiochemical yield. The final mixture was allowed to dry. The residue was further dissolved in 2 ml of NaOH (0.1 N).

About 0.2 ml of HCl (1 M) was used to precipitate the RIRB following centrifugation, where the resultant precipitate was then dissolved in 2 ml of phosphate buffer (pH 7.3). Furthermore, the purification of RIRB from the unreacted ^{131}I was achieved by reprecipitation method several times [34]. In order to determine the radiochemical yield of the product, each set of RIRB and supernatant was detected individually for radioactivity.

Paper chromatography (PC) method was adopted to assess the in-vitro stability and radiochemical yield of RIRB where fresh mixture of methanol: chloroform (1:1 *v*/v) was selected as a developing agent in the preparation of Whatman paper (number 1) strips. On each paper strip (1 cm × 13 cm), 1–2 μL of the prepared RIRB was seeded 2 cm above the lower edge, evaporated and developed. RIRB developed to R_f value of 0.85 while, the free radioiodide (I^-) remained at the spotting point (R_f = 0–0.1), after full development, each strip was dried and cut into strips (1 cm) then counted in a well type A NaI (Tl) γ-ray scintillation counter (Scaler Ratemeter SR7, Nuclear Enterprises, Edinburgh, England) [35–37].

Different factors affecting the radioiodination process (reaction time and temperature, pH, amount of potassium iodate and rose bengal) were studied and optimization was carried out to reach the highest radiochemical yield. Each factor was studied in triplicates.

Evaluation of liver uptake

In this study, the presence of the radioactive dye in the liver provides a mean of scanning the liver moreover its excretion may be utilized to study the hepatic function [20–24]. Therefore, the selective uptake of RIRB by the liver supported its usage for assessment of liver function as RIRB liver uptake diminished significantly in case of hepatic damage. The hepatoprotective activity of AD from the optimum NLC formula following TAA induced hepatic injury in mice was assessed by determination of RIRB liver uptake following intravenous injection of the radioiodinated indicator. For the achievement of this objective, the percent of injected dose per gram organ (% ID/g ± SEM) was calculated at each time interval post I.V injection of radioiodinated rose bengal. In addition, the liver uptake/Blood (T/B) ratio is calculated at different time intervals being the key parameter to assess the selectivity and potentiality of the liver to RIRB [38].

The biodistribution study of RIRB was performed in accordance with the guidelines set by the Egyptian Atomic Energy Authority (EAEA) for animal experiments. The experimental protocol was accredited by Research Ethics Committee, Faculty of Pharmacy, Cairo University (REC-FOPCU).

Forty-five Swiss albino healthy mice of weight ranged between 20 and 25 g each were accommodated under established state of temperature, humidity and light for 7 days in polypropylene cages to decrease the variation with a free access to criterion diet and water ad libitum. The mice were erratically assigned to three groups of fifteen mice, three mice for each time interval [39, 40], as cited in (Table 2). Animals received (10 mg/kg/day, IP) dextrose, water and ringer lactate solutions to avoid renal failure, hypoglycemia and electrolyte disturbance till the end of the experiment.

An amount equivalent to 3.7 MBq present in 100 μl RIRB was injected intravenously (I.V.) via the mouse tail vein which is then anesthetized by chloroform and weighted [38, 41]. In-vivo biodistribution of RIRB in mice at different time intervals (0.25, 0.5, 1, 2 and 3 h post I.V injection) were determined.

Samples of fresh blood were withdrawn, in addition, mice organs/tissues were incised, rinsed with normal saline then all were weighted and recorded for their radioactivity as well as the background was counted in a well-type NaI(Tl) crystal coupled to SR-7 scaler-ratemeter [42]. The total blood radioactivity level was computed considering blood to constitute

Table 2 Dosage regimen of the different Swiss Albino mice groups used for the evaluation of liver uptake following IV injection of RIRB

Group number	Dosage regimen
1 [Placebo]	Mice administered (2 mL/kg) saline intraperitoneally (IP) once then 5 mL/kg oral saline daily for 3 successive days.
2 [(TAA) induced Hepatotoxicity]	Mice administered (300 mg/kg) TAA intraperitoneally (IP) once
3 [Treatment]	On the 1st day, mice received 300 mg/kg intraperitoneal TAA once and then 10 mg/kg orally from AD-loaded formula (F12) administered daily for 3 successive days after 24 h following TAA injection.

7% of total mice weight [43]. Percent of injected dose per gram organ (% ID/g ± SEM) for bone and muscle were also calculated [44] in a population of three mice at each time interval for each organ.

Statistical analysis

The obtained results were subjected to statistical analysis using one-way analysis of variance (*ANOVA*) followed by the least-significant difference (LSD) test using SPSS® software version 20 (SPSS Inc., Chicago, USA). $p < 0.05$ was the selected level of significance difference.

Results and discussion

Lipid screening and selection of lipid matrix

A huge versatility of solid lipids and liquid lipids are available as matrix lipids for NLC production, differ in their origin including natural, semi-synthetic and synthetic lipids with various structures, e.g. fatty acids, waxes and steroids, triglycerides, partial glycerides. Owing to the great impact of the composition of lipids matrix on the performance of the NLC system, hence they must be carefully chosen [45].

The proper selection of lipid matrices with less organized forms or lipids exposing a diminished liability for crystallization was the main aim for the preparation of NLCs as to diminish the ejection of the drug during storage. Moreover, selection of biodegradable and physiologically lipids is the key solution for the issue of biocompatibility and possible toxicities that arise from most of the lipids. In addition, the drug encapsulation efficiency and payload can be enhanced by selecting lipids of low crystallinity in which the drug displays a high solubility [46–48].

Based on the preferential solubility of AD in solid and liquid lipids as depicted from (Fig. 1a), it is clear that AD exhibits significantly ($p < 0.05$) higher solubility of 90 mg/g in Precirol ATO-5 (Glyceryl palmitostearate) made up of a mixture of mono-, di-, and tri-acylglycerols of palmitic (saturated C_{16}) and stearic (saturated C_{18}) fatty acids followed by 80 mg/g in Compritol 888 (Glyceryl behenate) a blend of different esters of behenic acid (saturated C_{22}) with glycerol, the mixture predominantly contains the diester glyceryl dibehenate [49].

It is well known that solid lipids of long hydrocarbon chain ($>C_{12}$) are characterized by lower HLB values and higher solubilizing power for AD [26]. Moreover, the utilization of oils and fats which are composed of mixtures of mono-, di- and triacylglycerols rather than monoacid triacylglycerols and comprising fatty acids differ in their degree of unsaturation and chain length leads to an increase in the drug solubility, despite they explicit a low drug charging capacity as the melting point of these lipids decreases with the degree of unsaturation and increases with the length of the fatty acid chain [50].

Hence the nature of the lipid is a critical concern because lipids casting particles in a highly organized and perfect manner (e.g., monoacid triacylglycerols) predispose to drug dislodgment during shelf time [26]. Moreover, Precirol ATO-5 grants a considerable space to accommodate the drug due to its ability to form less organized crystalline form as it is composed of fatty acids which vary in their chain length (palmitic C_{16} and stearic C_{18}), so that Precirol ATO-5 was selected as the solid lipid matrix for the preparation of AD encapsulated NLCs. Müller et al. have stated that the degree of crystallinity of solid lipid decreased upon the incorporation of oil, therefore decreasing by turn the drug expulsion [46]. Regarding the liquid lipids, it was found that AD had the maximum solubility (120 mg/g) in Capmul MCM (mono-diglyceride of medium chain fatty acids (mainly caprylic and capric) followed by (105 mg/g) for Capryol-90 (propylene glycol monocaprylate), (Fig. 1b).

In the current study, different NLC formulae charged with AD were prosperously processed adopting solvent diffusion technique utilizing Precirol ATO-5 (solid lipid) together with Capmul MCM (Liquid lipid) in a ratio of (3:1) with a lipid mixture concentration of 2 and 5% *w/v* in presence of SAA (Cremophor RH 40 or Pluronic F68) with or without egg yolk lecithin.

In-vitro characterization of the prepared AD-loaded NLCs

Entrapment efficiency percent (E.E%)

The entrapment efficiency percent (E.E%) of the different formulated AD-loaded NLCs are cited in (Table 1), E.E%

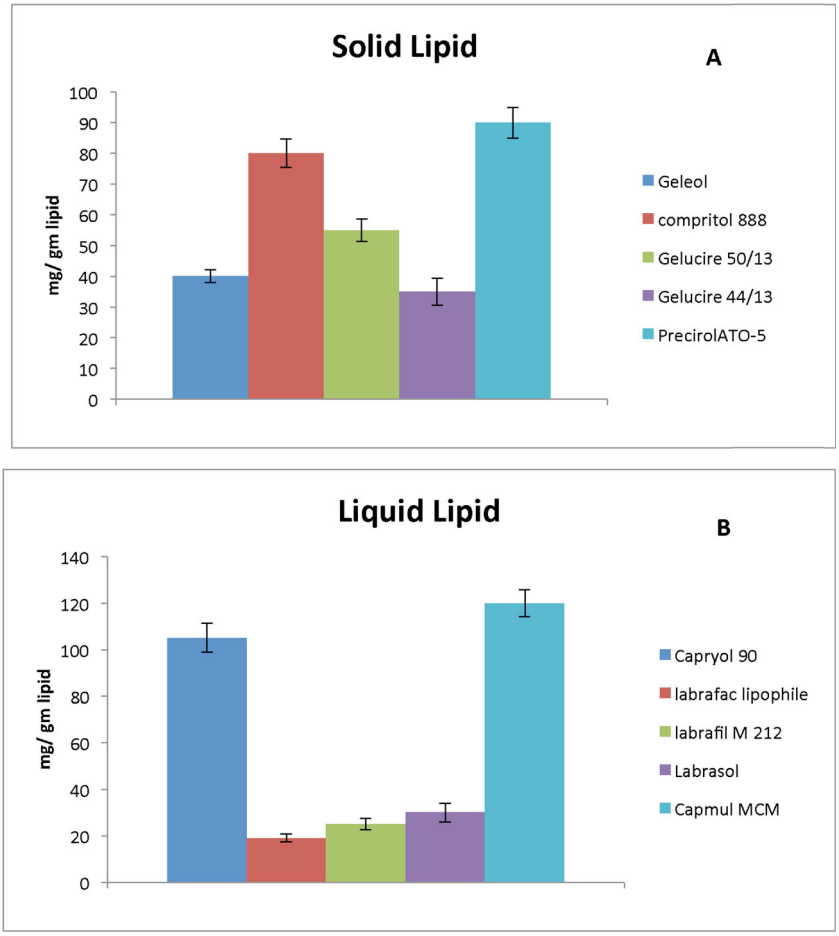

Fig. 1 Screening test of AD solubility in: **a** Solid lipids and **b** Liquid lipids

ranged from 5.5 ± 0.24 to 90.5 ± 0.21%. In favor of optimizing the encapsulation of AD, the aforementioned factors were appraised as follows:

Effect of total lipid concentration It was found that varying the total lipid concentration in the fabricated nanoparticles from 2 to 5% *w/v* showed a significant effect ($p < 0.05$) on the entrapment of AD, (Fig. 2a). For instance, E.E% (7.95 ± 0.2%) for formula F6 was significantly increased to (50.35 ± 1.3%) in F8 with increasing the lipid content from 2 to 5%w/v. According to Poonia et al., the increment in the total lipid matrix amount exposes an improvement in entrapment efficiency of NLCs. The higher lipid content predisposes to a depression in the drug expulsion leading to higher entrapment efficiency. These results could be justified by the great affection of AD to the previously selected Precirol ATO-5 and Capmul MCM after preliminary screening test [14].

The entrapment efficiency and drug loading capacity (LC) were highly influenced by polymorphism and level of crystallinity of the lipid matrix. During the formulation of NLCs all or at least part of the lipid matrix recrystallizes in the form of a less or unstable α-polymorphic form or in the metastable β'-polymorphic form, but they have a tendency to be transformed to the most stable β- form [51]. As the alignment process and conversion to the more stable polymorphic forms proceeds, there is a subsequent decrease in the number of defects in the lipid network, i.e., the configuration of β'/β forms diminishing the drug encapsulation.

Generally, the rate of this transfiguration is lower for long-chain triglycerides as Precirol ATO-5 compared to short-chain triacylglycerols [52]. In order to achieve NLC with aspired properties, it very critical to select the optimal lipid content. Furthermore, the presence of liquid lipid in which the drug shows higher solubility in the form of nano-oil portions in the solid grid leading to many deformations in the crystal lattice predisposing to an increase in the total drug loading capacity. Thus increasing the total lipid mixture content leading to massive voids and imperfections in the lipid network ready for the accommodation of much more drug molecules resulting in higher entrapment efficiency [53, 54].

Effect of surfactant concentration The inclusion of surfactants in NLC formulations aims to disperse one immiscible phase into another. The surfactants tend to lessen the tension between the lipid phase and aqueous phase, which subsequently generates finer particles, hence increasing the surface area of lipid

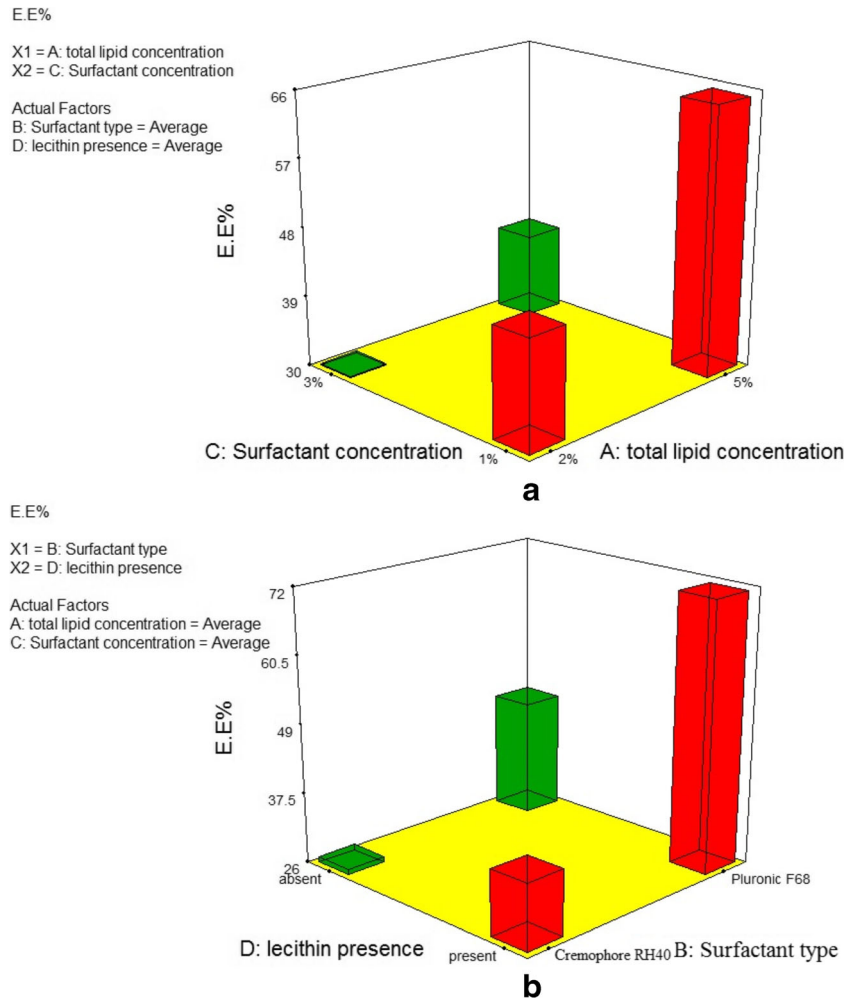

Fig. 2 Effect of different variables on E.E%; **a** Lipid concentration and SAA concentration and **b** SAA type and Presence of lecithin

droplets [55]. Moreover, (Fig. 2a) demonstrates that the entrapment of NLCs significantly decreased ($p < 0.05$) upon increasing the surfactant concentration from 1 to 3% *w/v*. For example, results of E.E% decreased significantly from 34.70 ± 2.4% in F2 to 7.95 ± 0.2% in F6 respectively. This might be attributed to the existence of greater amount of surfactant resulting in the formation of smaller particles entrapping lower drug [31, 56].

Effect of surfactant type The choice of the suitable surfactant is very essential for NLCs preparation. In the current study, two non-ionic surfactants were used; Cremophor RH40 and Pluronic F68. The most proper Hydrophilic-lipophilic balance (HLB) value for the manufacture of stable O/W emulsion is 12–16. The HLB value of Cremophor RH40 (PEG-40 hydrogenated castor Oil) ranges between (14–16), while that of Pluronic F68 (Polyoxyethylene-Polyoxypropylene block copolymer) equals to 29. A noticeable variation in emulsification power was evident upon using the previously mentioned surfactants despite having HLB values greater than 10, (Fig. 2b).

It is clear that the E.E% of NLCs fabricated using Pluronic F68 (90.55 ± 0.2% for formula F12) was significantly ($p < 0.05$) greater than those formulated in case of Cremophor RH40 (55.05 ± 1.6% for formula F4), Similar results were observed by Das et al., where Pluronic F68 resulted in increasing the E.E% of Clotrimazole, a highly lipophilic drug, compared to Cremophor EL [31].

Various factors rather than HLB value had also a great impact on the magnitude of E.E% like the length and structure of hydrocarbon chain of surfactants, Cremophor RH40 composed mainly of castor oil, a triglyceride in which each of its three hydroxyl groups esterifies with a long-chain unsaturated fatty acid (hydroxylated 12-hydroxy, 9-octadecenoic acid) known as ricinoleic acid. Glycerol ethoxylates and polyethylene glycols derivatives of long chain ricinoleic acid imparting poor stabilizing efficiency confirmed by the lower E.E% at higher concentration especially in the presence of low lipid concentration, (Table 1). On contrary, Pluronic F68 being block copolymer is composed of polyoxypropylene oxide as a hydrophobic segment and polyoxyethylene oxide as a hydrophilic segment [57, 58]. This huge polymeric grid of polyoxyethylene oxide (hydrophilic segment) orients in external phase, while polyoxypropylene oxide (hydrophobic

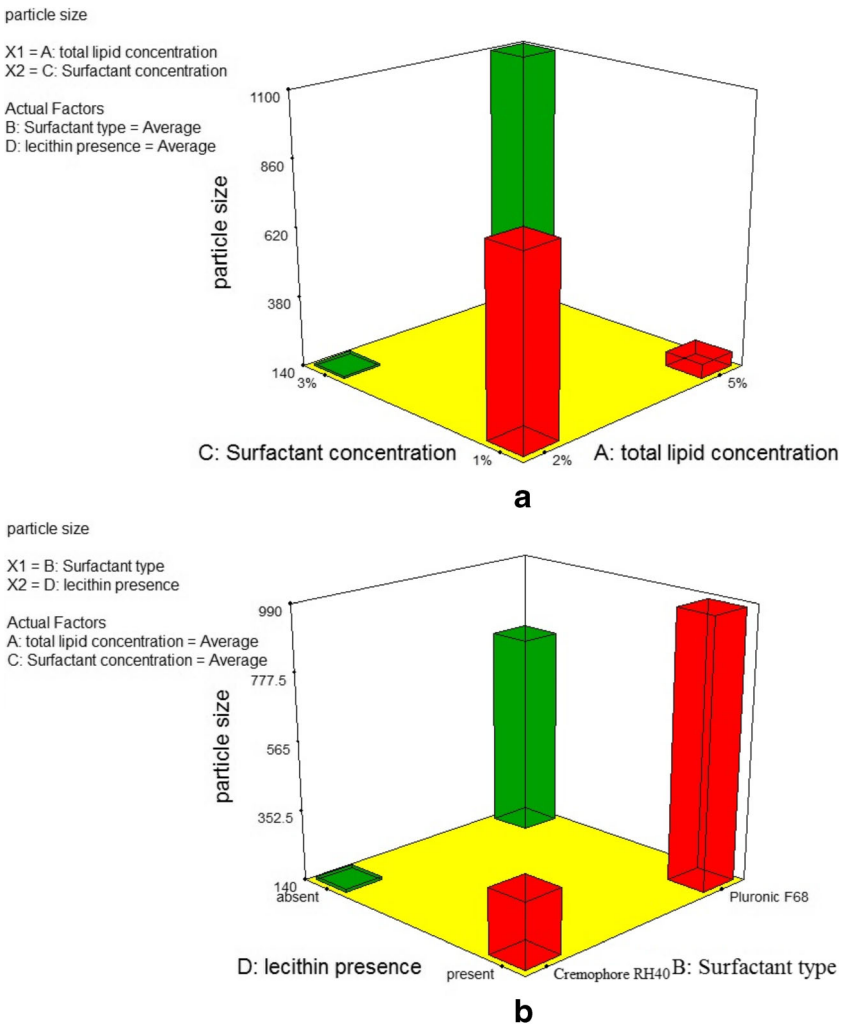

Fig. 3 Effect of different variables on particle size; **a** Lipid concentration and SAA concentration and **b** SAA type and Presence of lecithin

segment) settles at interface and leading to more steric stabilization of NLC permitting larger surface area for accommodation of the drug [59].

Effect of presence of lecithin It was depicted that the E.E% of AD within the fabricated NLCs containing lecithin was significantly ($p < 0.05$) greater than those fabricated without lecithin ($90.55 \pm 0.2\%$ in formula F12 compared to $5.53 \pm 0.2\%$ in formula F5, respectively), (Fig. 2b). This might be attributed to the effect of lecithin in improving the emulsification power of the surfactants, hence magnifying the prepared system stability. Furthermore lecithin was primarily allocated at the interface between the aqueous phase and oil phase resulting in an increase in the drug loading capacity [60].

Vesicle size, zeta potential and polydispersity index (PDI) determination

As represented by (Table 1), the size of the fabricated NLC formulae ranged from (59.1 ± 1.1 to 940 ± 59.8 nm), where F5 showed the smallest particle size, while F16 showed the largest one. Polydispersity index (PDI) values ranged from (0.21 ± 0.048 to 0.56 ± 0.2) that reveal the homogeneity in particle size distribution [31].

The value of zeta potential gives an indication to the extent of repulsion between NLC particles and therefore their future stability [61, 62]. Results shown in (Table 1) indicate that zeta potential values were in the range of (-7.89 ± 1.1 mV to -26.45 ± 0.21 mV) which might be due to the presence of fatty acid residue in the prepared formulae. The influence of different variables on the particle size was explained as follows:

Effect of total lipid concentration It was found that varying the concentration of lipid matrix from 2 to 5% *w*/*v* displayed a significant ($p < 0.05$) decrease in particle size, (Fig. 3a). This was in accordance with Gardouh et al. who mentioned that during the preparation of nanostructured lipid carriers, the incorporation of liquid lipid to solid lipid has a propensity to develop small particles, as a result of increasing the matrix molecular mobility after liquid oil inclusion [63].

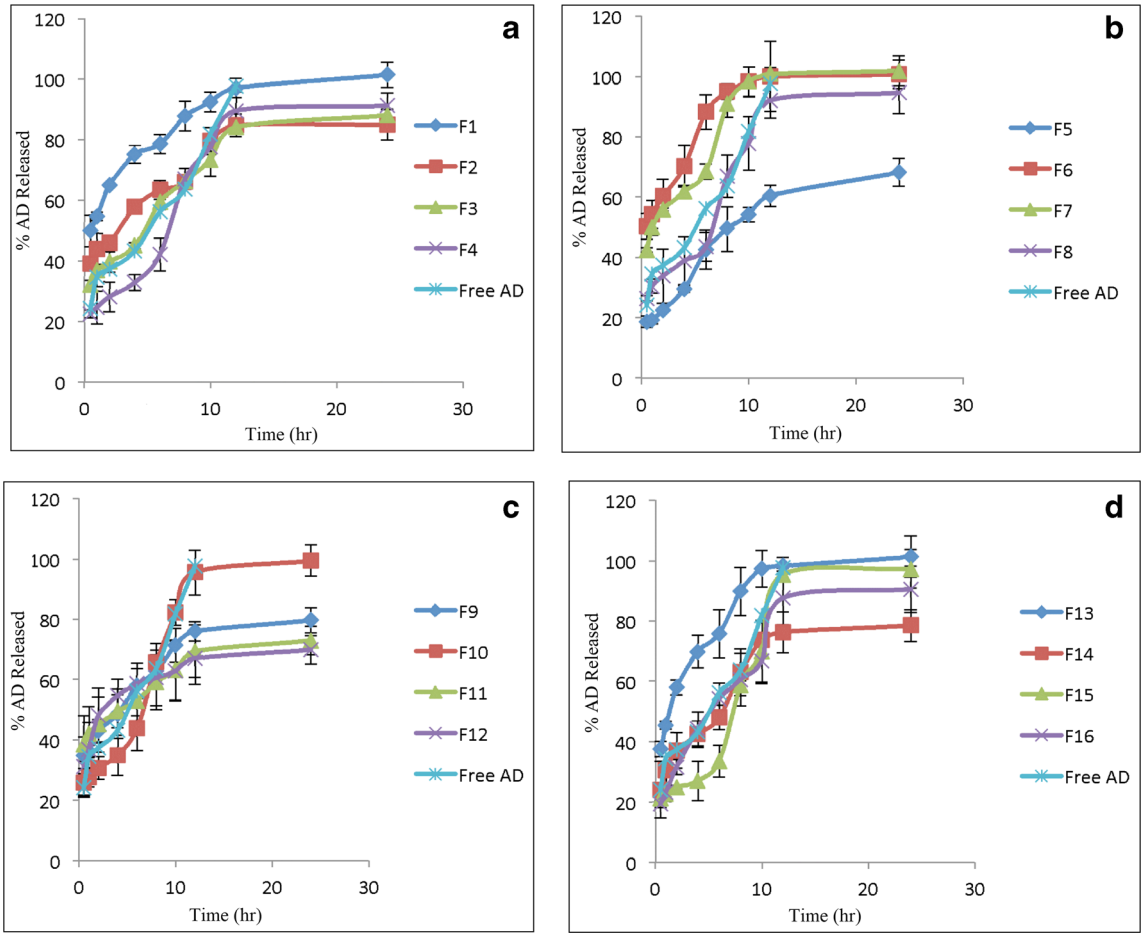

Fig. 4 In-vitro release profiles of AD from the prepared AD-loaded NLC formulae, (**a**) formulae contain 1% Cremophor RH40, (**b**) formulae contain 3% Cremophor RH40, (**c**) formulae contain 1% Pluronic F68 and (**d**) formulae contain 3% Pluronic F68.

Effect of surfactant concentration It is well known that NLCs containing higher surfactant concentration showed significantly ($p < 0.05$) lower particle size than those containing lower surfactant concentration. For example, the particle size of F5 fabricated with 3% *w/v* Cremophor RH40 was found to be equal to 59.15 ± 1.1 nm compared to 132.50 ± 11.2 nm in formula F1 containing 1% w/v Cremophor RH40. This might be attributed to the resulted reduction in the interfacial tension of the lipid droplets leading to the disruption of the lipid droplets into smaller ones. Furthermore, higher surfactant concentration leads to the presence of enough surfactant to coat and stabilize the fine droplets of the lipids and hinder the coalescence of the nano-sized emulsion globules [56, 64].

There was a significant difference ($p < 0.05$) in particle size between formulae prepared using either 1 or 3% w/v surfactant, (Fig. 3a), where the fabricated nanoparticles utilizing (1% w/v) exhibit a diminished repulsion force between the particles forming agglomerates throughout storage.

Effect of surfactant type The particle size of AD-loaded NLC formulae prepared using Cremophor RH40 were significantly ($p < 0.05$) smaller in size (59.15 ± 1.1 nm for F5), ($p < 0.05$), compared to formulae prepared using Pluronic F68 (144.71 ± 5.6 nm for F13) as illustrated in (Fig. 3b). Higher HLB values more than 20 in Pluronic F68 was the keystone for globule aggregation and production of large particle size while Cremophor RH40 whose HLB equals to a range of 12–14 gave rise to stable NLCs as the most proper Hydrophilic-lipophilic balance (HLB) value for the manufacture of stable O/W emulsion lies between 12 and 16 [59].

Effect of presence of lecithin Results declared that the presence of lecithin showed a significant influence ($p < 0.05$) on the particle size of the prepared formulae, (Fig. 3b). As previously mentioned that lecithin was chiefly allocated at the interface between the aqueous phase and the oily phase and leading to incorporation of more drug resulting in bigger particles [60].

In-vitro AD release

Drug release pattern from the prepared lipid nanocarriers relied mainly on the drug incorporation mode into the lipid matrix (i.e. homogeneous drug distribution within the matrix,

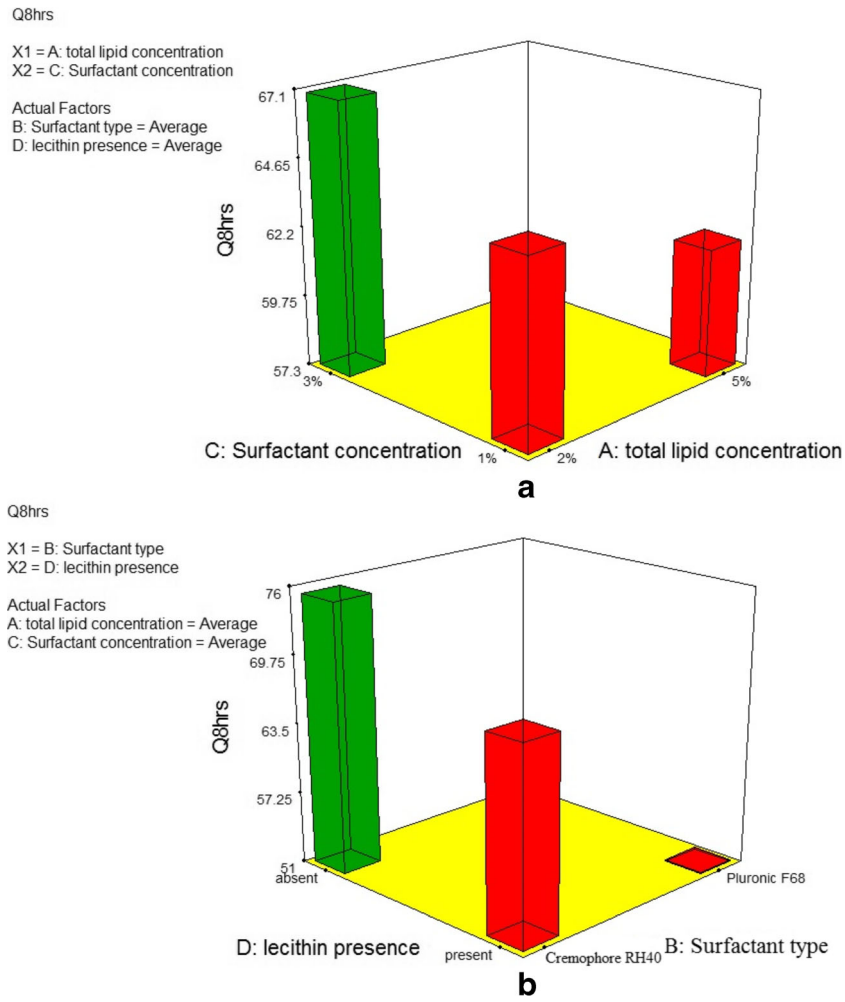

Fig. 5 Effect of different variables on Q8hrs; **a** Lipid concentration and SAA concentration and **b** SAA type and Presence of lecithin

drug-enriched shell or drug-enriched core) [46–48]. In addition, other factors like drug lipid solubility, surfactant composition, formulation temperature and amount of oil included in the lipid grid are among the factors affecting the in-vitro release pattern [53].

Figure 4 (A-D) displays in-vitro AD release profiles from the different prepared NLCs, where AD release exhibited a dual release pattern; a burst phase at the beginning of release which might be due to the allocation of the drug in the external shell, while the second phase extended up to 24 h due to the presence of enclosed drug within the core

In addition, the preparation method of AD-NLC might also explain the proposed mechanism of AD release as throughout the recrystallization process, on cooling lipids tend to solidify very fast forming the core where the oil is randomly scattered through it. Part of the oil might diffuse to the external shell of the particles enclosing some of the drug explaining the initial burst phase followed by slower degradation of the lipid grid, giving rise to an extended AD release representing the release of the rest of drug being enclosed within the core of the particles [65–67].

As illustrated in (Fig. 4), results of Q8hrs in-vitro AD release from the different prepared NLCs formulae ranged from 49.43 ± 7.37 to $94.91 \pm 2.55\%$. All studied variables had no significant effect ($p > 0.05$) on Q8hrs except for the surfactant type (Fig. 5), where Pluronic F68 showed a significant lower release ($p < 0.05$) compared to Cremophor RH40. This might be attributed to the stabilizing properties of Pluronic F68 as previously discussed permitting larger surface area for drug accommodation. Thus, a lower rate of drug expulsion can be accomplished in favour of this collective hydrophilic/hydrophobic interaction with NLCs offering greater stability [57, 58].

Depending on the aforementioned results, NLC formula (F12) comprises of Precirol ATO-5 and Capmul MCM (3:1) as the lipid matrix (5%*w*/*v*) together with Pluronic F68 as surfactant in a concentration of 1%w/v in presence of 1%w/v egg yolk lecithin attained the optimum properties for picking the desired responses; maximum E.E%, minimum globule size and Q8hrs with a desirability value of approximately 0.757. Further evaluation tests were carried out on the optimum lyophilized formula (F12) as follows:

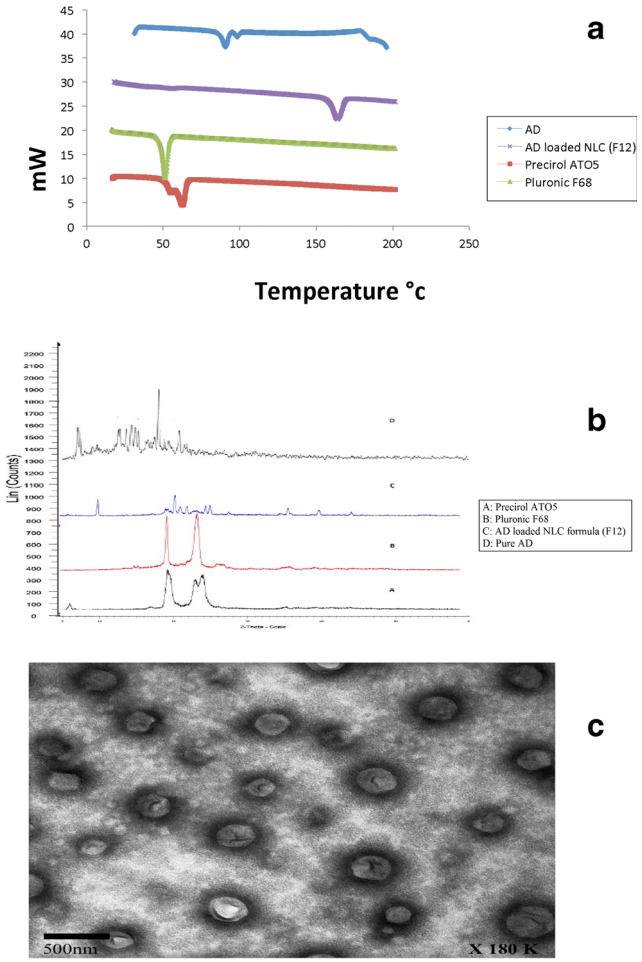

Fig. 6 In-vitro characterization of the optimum AD-loaded NLC formula (F12) via: (**a**) DSC, (**b**) X-ray Diffractometry and (**c**) TEM

In-vitro characterization of the desired AD-charged NLC formula

Freeze dried AD-NLC formula (F12) displayed spontaneous dispersion upon reconstitution with water. Moreover, no signs for drug precipitation or lump formation.

Differential scanning calorimetry (DSC)

DSC thermograms of pure AD, Precirol ATO-5, Pluronic F68 as well as the optimum lyophilized AD-loaded NLC formula (F12), (Fig. 6a). DSC thermogram of pure AD revealed an acute pointed distinctive endotherm at approximately 102 °C which is equivalent to its melting [5], while Precirol ATO-5 exhibited an endothemic peak at 62 °C corresponding to its melting point [26]. Pluronic F68 showed an endothermic peak at 51.2 °C [68].

DSC thermogram of lyophilized AD-loaded NLC formula (F12) exhibited no characteristic peak of AD suggesting the complete transaction of AD from a crystalline to amorphous form proposing good encapsulation of the drug within the nanolipid compartment during the preparation method and even after lyophilization [69, 70].

Further ceasing in the distinctive melting peak of the lipid matrix (Precirol ATO-5) which could be owed to the presence of less organized or destructed crystal lattice of lipid matrix in NLC formulae [26]. The Thermogram of lyophilized NLC also revealed an endothermic peak at 163.5 °C which is equivalent to the melting point of the used cryoprotectant (mannitol).

X-ray diffractometry (XRD)

Figure 6b exhibits the X-ray diffractograms of pure AD, Precirol ATO-5, Pluronic F68, and the optimum lyophilized AD-loaded NLC formula (F12). Results of XRD revealed the crystallinity of Precirol ATO-5, Pluronic F68 and pure drug. AD crystallinity confirmed by multiple characteristic peaks at 2θ angles; 17.4° and 20.9° respectively. 2θ angles at 19.4°, 23.2° and 24.1° were the distinct peaks for Precirol ATO-5 revealing the crystalline state of Precirol ATO-5, while two distinct peaks of Pluronic F68 at 2θ angles; 19.27° and 23.4 were observed. The transformation of AD, Precirol ATO-5 and Pluronic F68 to the amorphous form in the optimum NLC formula (F12) was further confirmed by the absence of their characteristic peaks, as shown in (Fig. 6b), [5]. The peaks appeared in the diffractogram of lyophilized NLC might be referred to the existence of mannitol as cryoprotectant throughout lyophilization process having intense peaks at 10°, 20°, 25°, 35–45° [71].

Transmission electron microscopy (TEM)

The production of nano-structured lipid carrier after the hydration of the lyophilized powder of the optimum AD-loaded NLC formula (F12) could be confirmed using TEM technique. As exploited in (Fig. 6c), spherical soft shaped lipid nanoparticles were noticed deprived from any crystals for drug figuring out to the complete conversion of the drug to the amorphous form as previously illustrated by DSC and XRD data.

Stability studies

Nanodispersions can exhibit improved physical stability and extended shelf life via freeze-drying process. Results of stability study regarding E.E%, globule size, PDI and in-vitro AD release (Q8hrs) revealed a non-significant difference, ($p < 0.05$), between the freshly prepared formula and the reconstituted dispersions obtained from the stored lyophilized NLC formula (F12) suggesting good stability after lyophilization.

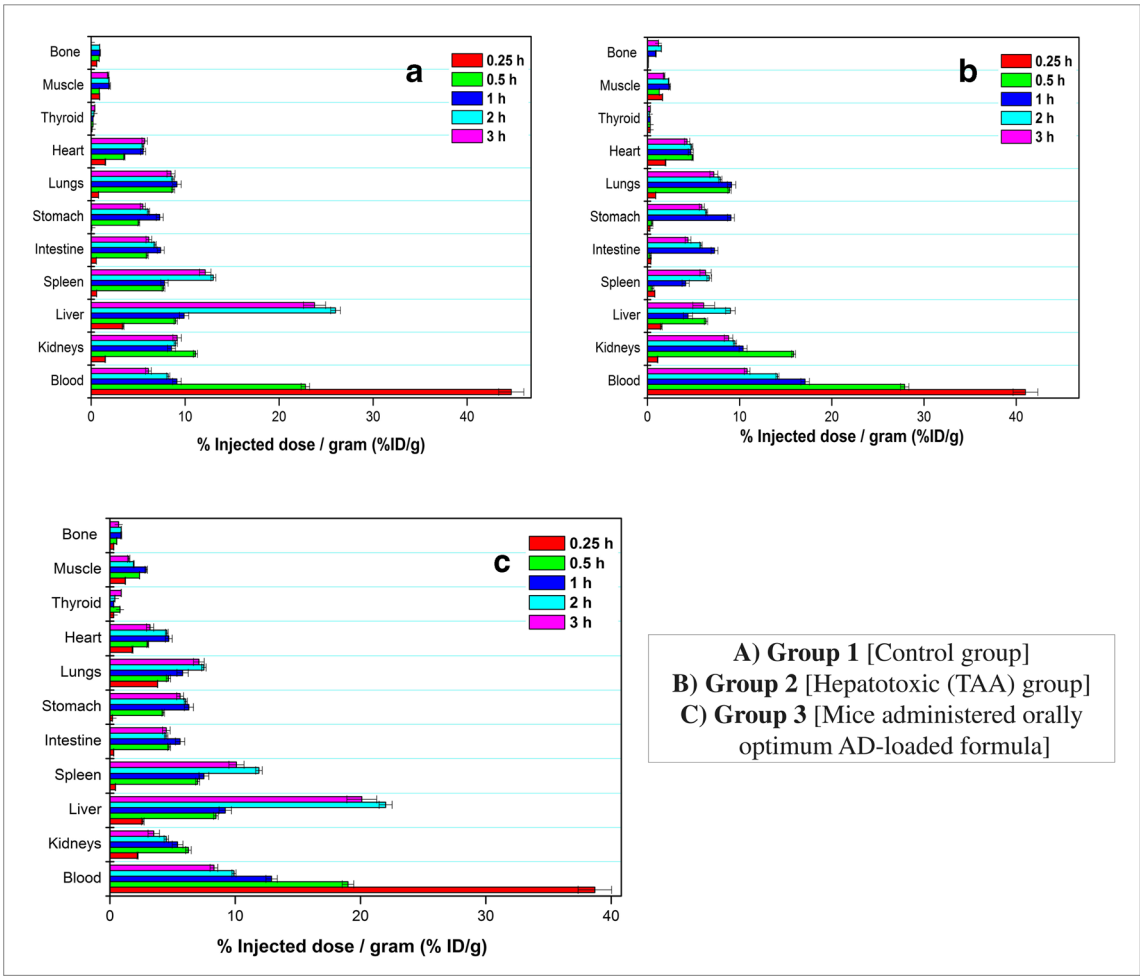

Fig. 7 In-vivo biodistribution of radioiodinated rose bengal in different groups of Swiss Albino mice at different time intervals post I.V. injection (%ID/g ± SEM, $n = 3$), (**a**) Group 1 [control], (**b**) Group 2 [hepatotoxic (TAA)] and (**c**) Group 3 [treatment (mice administered orally optimum AD-loaded formula)]

In-vivo studies of the optimum AD-loaded NLC formula

Radiochemical yield of radioiodinated rose bengal

The highest radiochemical yield of RIRB was about 91.5 ± 0.3%. This grand yield could be reached via utilizing 10 mg of RIRB and 0.3 mg of potassium iodate. Radiolabeling reaction was performed at 80 °C for 45 min. After further purification by effective reprecipitation method, the contamination of free iodide can be reduced to be less than 1.5% by reprecipitating the RIRB thrice.

In-vitro stability of radioiodinated rose bengal

In-vitro stability of RIRB is very essential for the detection of the proper utilization period in order to prevent the production of undesired radioactive products superseding its decomposition during storage. RIRB showed in-vitro stability up to 24 h which is sufficient to perform the in-vivo biodistribution study [72].

Evaluation of liver uptake

The in-vivo biodistribution of RIRB was assessed in the three previously mentioned groups of mice. The percent injected dose/g (% ID/g) was calculated at each time interval post I.V injection of RIRB. The (% ID/g ± SEM) for bone and muscle were calculated and found to be equal to 10 and 40% of the total body weight, respectively. Biodistribution results of RIRB in different body tissues, fluids and organs are illustrated in (Fig. 7) (A, B and C for Groups 1, 2 and 3, respectively). RIRB showed selective and significant higher ($p < 0.05$) accumulation in the liver, compared to other organs, in Groups (1 and 3) contrary to Group 2.

A comparison of the liver uptake of RIRB between the three different groups of Swiss Albino mice was depicted

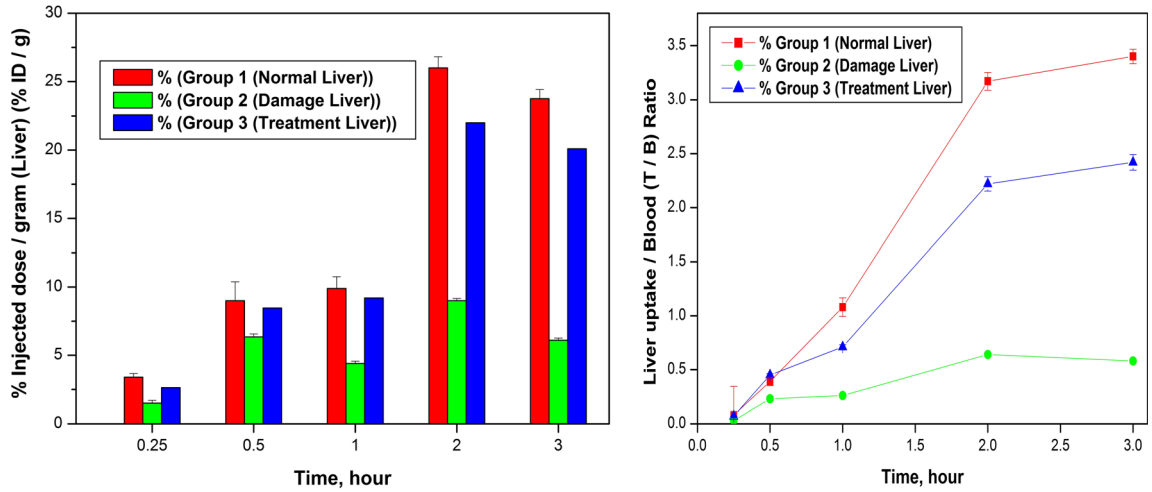

Fig. 8 Comparison of liver uptake and T/B ratio of radioiodinated rose bengal in different groups of Swiss Albino mice at different time intervals post I.V. injection. (%ID/g (liver) ± SEM, $n = 3$)

in (Fig. 8). It is clear that Group 1 (control group) exhibited the highest significant ($p < 0.05$) liver uptake where (% ID/g) after 2 h post I.V injection was 26 ± 0.03%. Concerning the least liver uptake of RIRB, a value of 9 ± 0.01% ID/g was obtained from the hepatotoxic group (Group 2). A significant increase in liver uptake, ($p < 0.05$) compared to the hepatotoxic group was achieved from Group 3, where % ID/g after 2 h post I.V injection reached 22 ± 0.01%. The above discussed results confirmed the effectiveness of the optimum AD-loaded formula F12 as a successful nano-carrier system for the oral targeted delivery of AD to the liver.

Similarly, after 2 h post I.V injection of RIRB, the liver uptake/Blood (T/B) ratio were significantly higher in groups 1 and 3 (3.17 ± 0.081 and 2.22 ± 0.067 respectively) compared to Group 2 (0.64 ± 0.017), ($p < 0.05$), confirming the selectivity and potentiality of RIRB towards the liver. Besides, the in-vivo stability of RIRB could be evidenced by lower values of thyroid uptakes among the three groups [42].

Conclusion

AD-loaded NLC optimized formula (F12) consisted of Precirol ATO-5 and Capmul MCM (3:1) as the lipid matrix (5% *w/v*) together with Pluronic F68 as surfactant (1% w/v) and egg yolk lecithin (1% w/v) exhibited vesicle size of 240.2 nm ± 2.5 and E.E% of about 90.5% ± 0.2. The optimized stable lyophilized NLC formula succeeded to protect the liver against chemically induced thioacetamide damage confirmed by higher liver uptake/Blood (T/B) ratio of 2.22 ± 0.067 following IV injection of RIRB. Therefore, NLC could be considered as prosperous oral targeting delivery system of the antiviral drug Adefovir Dipivoxil to the liver.

Compliance with ethical standards

Conflict of interest The authors declare that they have no conflict of interest.

References

1. Jiang JT, Xu N, Zhang X-y, Wu C-p. Lipids changes in liver cancer. J Zhejiang Univ Sci B. 2007;8:398–409.
2. Hadziyannis SJ, Tassopoulos NC, Heathcote EJ, Chang T-T, Kitis G, Rizzetto M, et al. Adefovir Dipivoxil for the treatment of hepatitis B e antigen–negative chronic hepatitis B. N Engl J Med. 2003;348:800–7.
3. Marcellin P, Chang TT, Lim SG, Tong MJ, Sievert W, Shiffman ML, et al. Adefovir Dipivoxil for the treatment of hepatitis B e antigen–positive chronic hepatitis B. N Engl J Med. 2003;348:808–16.
4. Lee WA, Martin JC. Perspectives on the development of acyclic nucleotide analogs as antiviral drugs. Antivir Res. 2006;71:254–9.
5. Dodiya S, Chavhan S, Korde A, Sawant KK. Solid lipid nanoparticles and nanosuspension of adefovir dipivoxil for bioavailability improvement: formulation, characterization, pharmacokinetic and biodistribution studies. Drug Dev Ind Pharm. 2013;39:733–43.
6. Carmona-Ribeiro AM. Biomimetic nanoparticles: preparation, characterization and biomedical applications. Int J Nanomedicine. 2010;5:249–59.
7. Abdelbary GA, Amin MM, Zakaria MY, El Awdan SA. Adefovir dipivoxil loaded proliposomal powders with improved hepatoprotective activity: formulation, optimization, pharmacokinetic, and biodistribution studies. J Liposome Res. 2018;28:259–74.
8. Shah NV, Seth AK, Balaraman R, Aundhia CJ, Maheshwari RA, Parmar GR. Nanostructured lipid carriers for oral bioavailability enhancement of raloxifene: design and in vivo study. J Adv Res. 2016;7:423–34.
9. Ghasemiyeh P, Mohammadi-Samani S. Solid lipid nanoparticles and nanostructured lipid carriers as novel drug delivery systems: applications, advantages and disadvantages. Res Pharm Sci. 2018;13:288–303.
10. Radtke M, Souto EB, Müller RH. Nanostructured lipid carriers: a novel generation of solid lipid drug carriers. Pharm Technol Eur. 2005;17:45–50.

11. Fang CL, Al-Suwayeh SA, Fang JY. Nanostructured lipid carriers (NLCs) for drug delivery and targeting. Recent Pat Nanotechnol. 2013;7:41–55.
12. Huang W, Dou H, Wu H, Sun Z, Wang H, Huang L. Preparation and characterization of nobiletin-loaded nanostructured lipid carriers. J Nanomater. 2017;54:1–10.
13. Khan S, Baboota S, Ali J, Khan S, Narang RS, Narang JK. Nanostructured lipid carriers: an emerging platform for improving oral bioavailability of lipophilic drugs. Int J Pharm Investig. 2015;5:182–91.
14. Poonia N, Kharb R, Lather V, Pandita D. Nanostructured lipid carriers: versatile oral delivery vehicle. Futur Sci OA. 2016;2:1–24.
15. Bayón-Cordero L, Alkorta I, Arana L. Application of solid lipid nanoparticles to improve the efficiency of anticancer drugs. Nanomaterials. 2019;9:E474.
16. Maker AV, Prabhakar B, Pardiwala K. The potential of intralesional rose bengal to stimulate T-cell mediated anti-tumor responses. J Clin Cell Immunol. 2015;06:1–6.
17. Qin J, Kunda N, Qiao G, Calata JF, Pardiwala K, Prabhakar BS, et al. Colon cancer cell treatment with rose bengal generates a protective immune response via immunogenic cell death. Cell Death Dis [Internet]. 2017 [cited 2019 May 24];8:e2584–e2584. Available from: http://www.ncbi.nlm.nih.gov/pubmed/28151483
18. Franchi R, Marabini A, Giorgetti PG, Santeusanio E. Use of the radioiodinated rose Bengal in the study of icterogenic hepatopathies. Ric Clin Lab. 1975;5:73–95.
19. Kawaguchi M, Soble AR, Berk JE. Studies with I131-labeled rose bengal I. Derivation of a technic for use in the differential diagnosis of jaundice. Am J Dig Dis. 1962;7:289–99.
20. Taplin GV, Meredith OM, Kade H. The radioactive (I131-tagged) rose bengal uptake-excretion test for liver function using external gamma-ray scintillation counting techniques. J Lab Clin Med. 1955;45:665–78.
21. Dyrbye MO, Christensen LK. Clinical value of the radioactive rose bengal liver function test. Acta Med Scand. 1960;167:239–43.
22. Gollin FF, Sims JL, Cameron JR. Liver scanning and liver function tests. JAMA. 1964;187:111–6.
23. Rajagopal KR. Radioactive rose bengal test of liver function. Probe (Lond). 1974;14:50–3.
24. Gamlen TR, Triger DR, Ackery DM, Fleming JS, Grant RW, Kenny RW, et al. Quantitative liver imaging using 131-I rose Bengal as an index of liver function and prognosis. Gut. 1975;16:738–43.
25. Hejri A, Khosravi A, Gharanjig K, Hejazi M. Optimisation of the formulation of β-carotene loaded nanostructured lipid carriers prepared by solvent diffusion method. Food Chem. 2013;141:117–23.
26. Patil-Gadhe A, Pokharkar V. Montelukast-loaded nanostructured lipid carriers: part I Oral bioavailability improvement. Eur J Pharm Biopharm. 2014;88:160–8.
27. Shete H, Patravale V. Long chain lipid based tamoxifen NLC. Part I: Preformulation studies, formulation development and physicochemical characterization. Int J Pharm. 2013;454:573–83.
28. Neupane YR, Sabir MD, Ahmad N, Ali M, Kohli K. Lipid drug conjugate nanoparticle as a novel lipid nanocarrier for the oral delivery of decitabine: ex vivo gut permeation studies. Nanotechnology. 2013;24:415102–13.
29. Abd-Elbary A, El-laithy HM, Tadros MI. Sucrose stearate-based proniosome-derived niosomes for the nebulisable delivery of cromolyn sodium. Int J Pharm. 2008;357:189–98.
30. Ranpise NS, Korabu SS, Ghodake VN. Second generation lipid nanoparticles (NLC) as an oral drug carrier for delivery of lercanidipine hydrochloride. Colloids Surf B Biointerfaces. 2014;116:81–7.
31. Das S, Ng WK, Tan RBH. Are nanostructured lipid carriers (NLCs) better than solid lipid nanoparticles (SLNs): development, characterizations and comparative evaluations of clotrimazole-loaded SLNs and NLCs. Eur J Pharm Sci. 2012;47:139–51.
32. Hupf HB, Wanek PM, O'Brien HA, Holland LM. Rapid radioiodination of rose bengal at room temperature. J Nucl Med. 1978;19:525–9.
33. O'Brien HJ, Hupf HB, Wanek PM. Instantaneous radioiodination of rose bengal at room temperature and a cold-kit therefor. U.S. Patent. US Dep Energy. 1981;4:298, 591.
34. Chen T-Y, Yeh S-J. Preparation of Iodine-131-labelled rose-bengal by radioactive exchange method. J Chin Chem Soc. 1964;11:94–101.
35. Ibrahim AB, Salem MA, Fasih TW, Brown A, Sakr TM. Radioiodinated doxorubicin as a new tumor imaging model: preparation, biological evaluation, docking and molecular dynamics. J Radioanal Nucl Chem. 2018;317:1243–52.
36. Shamsel-Din HA, Ibrahim AB. A novel radiolabeled indole derivative as solid tumor imaging agent: in silico and preclinical pharmacological study. J Radioanal Nucl Chem. 2017;314:2263–9.
37. Sakr TM, Ibrahim AB, Fasih TW, Rashed HM. Preparation and biological profile of ^{99m}Tc-lidocaine as a cardioselective imaging agent using ^{99m}Tc eluted from ^{99}Mo/^{99m}Tc generator based on Al–Mo gel. J Radioanal Nucl Chem. 2017;314:2091–8.
38. Ibrahim AB, Sakr TM, Khoweysa OMA, Motaleb MA, Abd El-Bary A, El-Kolaly MT. Radioiodinated anastrozole and epirubicin as potential targeting radiopharmaceuticals for solid tumor imaging. J Radioanal Nucl Chem. 2015;303:967–75.
39. Aburahma MH, Abdelbary GA. Novel diphenyl dimethyl bicarboxylate provesicular powders with enhanced hepatocurative activity: preparation, optimization, in vitro/in vivo evaluation. Int J Pharm. 2012;422:139–50.
40. Pawa S, Ali S. Liver necrosis and fulminant hepatic failure in rats: protection by oxyanionic form of tungsten. Biochim Biophys Acta. 1688;2004:210–22.
41. Fahmy AM, El-Setouhy DA, Ibrahim AB, Habib BA, Tayel SA, Bayoumi NA. Penetration enhancer-containing spanlastics (PECSs) for transdermal delivery of haloperidol: in vitro characterization, ex vivo permeation and in vivo biodistribution studies. Drug Deliv. 2018;25:12–22.
42. Ibrahim AB, Sakr TM, Khoweysa OMA, Motaleb MA, Abd El-Bary A, El-Kolaly MT. Formulation and preclinical evaluation of ^{99m}Tc–gemcitabine as a novel radiopharmaceutical for solid tumor imaging. J Radioanal Nucl Chem. 2014;302:179–86.
43. Motaleb MA, El-Kolaly MT, Ibrahim AB, Abd E-BA. Study on the preparation and biological evaluation of ^{99m}Tc–gatifloxacin and ^{99m}Tc–cefepime complexes. J Radioanal Nucl Chem. 2011;289:57–65.
44. El-Setouhy DA, Ibrahim AB, Amin MM, Khowessah OM, Elzanfaly ES. Intranasal haloperidol-loaded miniemulsions for brain targeting: evaluation of locomotor suppression and in-vivo biodistribution. Eur J Pharm Sci. 2016;92:244–54.
45. Mohammadi M, Pezeshki A, Abbasi MM, Ghanbarzadeh B, Hamishehkar H. Vitamin D3-loaded nanostructured lipid carriers as a potential approach for fortifying food beverages; in vitro and in vivo evaluation. Adv Pharm Bull. 2017;7:61–71.
46. Müller RH, Radtke M, Wissing SA. Solid lipid nanoparticles (SLN) and nanostructured lipid carriers (NLC) in cosmetic and dermatological preparations. Adv Drug Deliv Rev. 2002;54:S131–55.
47. Mehnert W, Mäder K. Solid lipid nanoparticles: production, characterization and applications. Adv Drug Deliv Rev. 2001;47:165–96.
48. Pardeike J, Hommoss A, Müller RH. Lipid nanoparticles (SLN, NLC) in cosmetic and pharmaceutical dermal products. Int J Pharm. 2009;366:170–84.
49. Aburahma MH, Badr-Eldin SM. Compritol 888 ATO: a multifunctional lipid excipient in drug delivery systems and nanopharmaceuticals. Expert Opin Drug Deliv. 2014;11:1865–83.

50. Hauss DJ. Oral lipid-based formulations. Adv Drug Deliv Rev. 2007;59:667–76.
51. Westesen K, Siekmann B, Koch MHJ. Investigations on the physical state of lipid nanoparticles by synchrotron radiation X-ray diffraction. Int J Pharm. 1993;93:189–99.
52. Souto EB, Müller RH. Lipid nanoparticles: effect on bioavailability and pharmacokinetic changes. In: Korting MS, editor. Drug Deliv handb Exp Pharmacol vol 197. Berlin: Springer; 2010. p. 115–41.
53. Hu FQ, Jiang SP, Du YZ, Yuan H, Ye YQ, Zeng S. Preparation and characteristics of monostearin nanostructured lipid carriers. Int J Pharm. 2006;314:83–9.
54. Jenning V, Mäder K, Gohla SH. Solid lipid nanoparticles (SLN) based on binary mixtures of liquid and solid lipids: a (1)H-NMR study. Int J Pharm. 2000;205:15–21.
55. Triplett MD, Rathman JF. Optimization of β-carotene loaded solid lipid nanoparticles preparation using a high shear homogenization technique. J Nanopart Res. 2009;11:601–14.
56. Liu J, Hu W, Chen H, Ni Q, Xu H, Yang X. Isotretinoin-loaded solid lipid nanoparticles with skin targeting for topical delivery. Int J Pharm. 2007;328:191–5.
57. Dai WG, Dong LC, Li S, Deng Z. Combination of Pluronic/vitamin E TPGS as a potential inhibitor of drug precipitation. Int J Pharm. 2008;355:31–7.
58. Ghosh I, Bose S, Vippagunta R, Harmon F. Nanosuspension for improving the bioavailability of a poorly soluble drug and screening of stabilizing agents to inhibit crystal growth. Int J Pharm. 2011;409:260–8.
59. Chen Y, Yang X, Zhao L, Almásy L, Garamus VM, Willumeit R, et al. Preparation and characterization of a nanostructured lipid carrier for a poorly soluble drug. Colloids Surf A Physicochem Eng Asp. 2014;455:36–43.
60. Zhuang CY, Li N, Wang M, Zhang XN, Pan WS, Peng JJ, et al. Preparation and characterization of vinpocetine loaded nanostructured lipid carriers (NLC) for improved oral bioavailability. Int J Pharm. 2010;394:179–85.
61. Das S, Chaudhury A. Recent advances in lipid nanoparticle formulations with solid matrix for oral drug delivery. AAPS PharmSciTech. 2011;12:62–76.
62. Freitas C, Müller RH. Effect of light and temperature on zeta potential and physical stability in solid lipid nanoparticle (SLN™) dispersions. Int J Pharm. 1998;168:221–9.
63. Gardouh AR, Faheim SH, Noah AT, Ghorab MM. Influence of formulation factors on the size of nanostructured lipid carriers and nanoemulsions prepared by high shear homogenization. Int J Pharm Pharm Sci. 2018;10:61.
64. Hu L, Tang X, Cui F. Solid lipid nanoparticles (SLNs) to improve oral bioavailability of poorly soluble drugs. J Pharm Pharmacol. 2004;56:1527–35.
65. Müller RH, Radtke M, Wissing SA. Nanostructured lipid matrices for improved microencapsulation of drugs. Int J Pharm. 2002;242:121–8.
66. zur Mühlen A, zur Mühlen E, Niehus H, Mehnert W. Atomic force microscopy studies of solid lipid nanoparticles. Pharm Res. 1996;13:1411–6.
67. Hu FQ, Jiang SP, Du YZ, Yuan H, Ye YQ, Zeng S. Preparation and characterization of stearic acid nanostructured lipid carriers by solvent diffusion method in an aqueous system. Colloids Surf B Biointerfaces. 2005;45:167–73.
68. Sun CZ, Lu CT, Zhao YZ, Guo P, Tian JL, Zhang L, et al. Characterization of the doxorubicin-pluronic F68 conjugate micelles and their effect on doxorubicin resistant human erythroleukemic cancer cells. J Nanomedicine Nanotechnol. 2011;2:2–7.
69. Pereira RR, Testi M, Rossi F, Silva Junior JOC, Ribeiro-Costa RM, Bettini R, et al. Ucuùba (Virola surinamensis) fat-based nanostructured lipid carriers for nail drug delivery of ketoconazole: development and optimization using box-behnken design. Pharmaceutics. 2019;11:284.
70. Yang G, Wu F, Chen M, Jin J, Wang R, Yuan Y. Formulation design, characterization, and in vitro and in vivo evaluation of nanostructured lipid carriers containing a bile salt for oral delivery of gypenosides. Int J Nanomedicine. 2019;14:2267–80.
71. Patel RJ, Patel ZP. Formulation optimization and evaluation of nanostructured lipid carriers containing valsartan. Int J Pharm Sci Nanotechnol. 2013;6:2077–86.
72. Nour SA, Abdelmalak NS, Naguib MJ, Rashed HM, Ibrahim AB. Intranasal brain-targeted clonazepam polymeric micelles for immediate control of status epilepticus: in vitro optimization, ex vivo determination of cytotoxicity, in vivo biodistribution and pharmacodynamics studies. Drug Deliv. 2016;23:3681–95.